Variational formalism for the Klein-Gordon oscillon

I. V. Barashenkov[1,2,*] and N. V. Alexeeva[1]

[1]*Centre for Theoretical and Mathematical Physics, University of Cape Town, Rondebosch 7701, South Africa*
[2]*Joint Institute for Nuclear Research, Dubna 141980, Russia*

(Received 22 August 2023; accepted 30 October 2023; published 21 November 2023)

The variational method employing the amplitude and width as collective coordinates of the Klein-Gordon oscillon leads to a dynamical system with unstable periodic orbits that blow up when perturbed. We propose a multiscale variational approach free from the blowup singularities. An essential feature of the proposed trial function is the inclusion of the third collective variable: a correction for the nonuniform phase growth. In addition to determining the parameters of the oscillon, our approach detects the onset of its instability.

DOI: 10.1103/PhysRevD.108.096022

I. INTRODUCTION

Oscillon is a classical solution describing a long-lived localized pulsating structure of finite amplitude. Oscillons play a role in the dynamics of inflationary reheating, symmetry-breaking phase transitions, and false vacuum decay [1–18]. They occur in the Einstein-Klein-Gordon equations [19–24], axion models [25–30], string phenomenology [31–33], and bosonic sector of the standard model [34–37]. The $(2+1)$-dimensional oscillons have been studied in the context of the planar Abelian Higgs theory [38,39].

Oscillons were discovered [40–43] in the $(3+1)$-dimensional Φ^4 model,

$$\Phi_{tt} - \Delta\Phi - \Phi + \Phi^3 = 0. \tag{1}$$

The model, together with its $(1+1)$-dimensional counterpart, remains a workhorse of quantum field theory [44–53] and cosmology [54]. Despite the apparent simplicity of Eq. (1), many properties of its oscillon solution have still not been fully understood [55].

Most of the mathematical analysis of oscillons has been carried out using asymptotic [55–57] and numerical techniques [1,42,43,55,58–61] while qualitative insights called on variational arguments. In Ref. [1], the Φ^4 oscillon was approximated by a localized waveform

$$\Phi = 1 + Ae^{-(r/b)^2}, \tag{2}$$

where $A(t)$ is an unknown oscillating amplitude and b is an arbitrarily chosen value of the width. (Reference [62] followed a similar strategy when dealing with the two-dimensional sine-Gordon equation.) Once the ansatz (2) has been substituted in the Lagrangian and the r-dependence integrated away, the variation of action produces a second-order equation for $A(t)$.

The variational method does not suggest any optimization strategies for b. Making $b(t)$ another collective coordinate—as it is done in the studies of the nonlinear Schrödinger solitons [63,64]—gives rise to an ill-posed dynamical system not amenable to numerical simulations. (See Sec. II below.)

With an obstacle encountered in $(3+1)$ dimensions, one turns to a $(1+1)$-dimensional version of the model for guidance. The analysis can be further simplified by considering oscillons approaching a symmetric vacuum as $x \to \pm\infty$. A physically relevant model of this kind was considered by Kosevich and Kovalev [65]:

$$\phi_{tt} - \phi_{xx} + 4\phi - 2\phi^3 = 0. \tag{3}$$

Unlike its Φ^4 counterpart, the oscillon in the Kosevich-Kovalev model satisfies $\phi \to 0$ as $x \to \pm\infty$ and oscillates, symmetrically, between positive and negative values. The asymptotic representation of this solution is

$$\phi = \frac{2\epsilon}{\sqrt{3}}\cos(\omega t)\,\mathrm{sech}(\epsilon x) - \frac{\epsilon^3}{24\sqrt{3}}\cos(3\omega t)\mathrm{sech}^3(\epsilon x) + O(\epsilon^5), \tag{4}$$

[*]Igor.Barashenkov@uct.ac.za

where $\omega^2 = 4 - \epsilon^2$ and $\epsilon \to 0$ [65]. Despite their difference in the vacuum symmetry, Eqs. (1) and (3) belong to the same, Klein-Gordon, variety and share a number of analytical properties.

The purpose of the present study is to identify a set of collective coordinates and formulate a variational description of the Klein-Gordon oscillon. A consistent variational formulation would determine the stability range of the oscillon, uncover its instability mechanism, and explain some of its properties such as the amplitude-frequency relationship. Using the $(1+1)$-dimensional Kosevich-Kovalev equation (3) as a prototype system, we transplant the idea of multiple timescales to the collective-coordinate Lagrangian method. With some modifications, our approach should remain applicable to oscillons in the $(3+1)$-dimensional Φ^4 theory and other Klein-Gordon models.

Before outlining the paper, three remarks are in order.

First, Eq. (3) can be seen as a truncation of the sine-Gordon model. The fundamental difference between the Kosevich-Kovalev oscillon and the sine-Gordon breather is that the latter solution is exactly periodic while the amplitude of the former one decreases due to the third-harmonic radiation. (When the amplitude of the oscillations is small, the radiation is exponentially weak though; hence the decay is slow).

Second, it is appropriate to mention an alternative variational procedure [66] where one not only chooses the spatial part but also imposes the time dependence of the trial function. For instance, one may set

$$\phi = A_0 \cos(\omega t) e^{-(r/b)^2}.$$

For a fixed ω, the action becomes a function of two time-independent parameters, A_0 and b. The shortcoming of this technique is that it does not allow one to examine the stability of the Klein-Gordon oscillon. Neither would it capture a slow modulation of the oscillation frequency—such as the one observed in numerical simulations of the Φ^4 model [42,58,60].

Our last remark concerns a closely related system, the nonlinear Schrödinger equation. The variational method has been highly successful in the studies of the Schrödinger solitons—scalar and vector ones, with a variety of nonlinearities and perturbations, and in various dimensions [63]. Several sets of collective coordinates for the Schrödinger solitons have been identified. It is the remarkable simplicity and versatility of the variational method demonstrated in the nonlinear Schrödinger domain that motivate our search for its Klein-Gordon counterpart.

The outline of the paper is as follows. In the next section we show that choosing the collective coordinates similar to the way they are chosen for the nonlinear Schrödinger soliton leads to singular finite-dimensional dynamics. A consistent variational procedure involving fast and slow temporal scales is formulated in Sec. III. We assess the approximation by comparing the variational solution to the "true" oscillon obtained numerically. Section IV adds remarks on the role of the third collective coordinate and the choice of the trial function, while an explicit construction of the oscillon with adiabatically changing parameters has been relegated to Appendix. Finally, Sec. V summarizes conclusions of this study.

II. SINGULAR AMPLITUDE-WIDTH DYNAMICS

A. Two-mode variational approximation

The variational approach to Eq. (3) makes use of its Lagrangian,

$$L = \frac{1}{2} \int (\phi_t^2 - \phi_x^2 - 4\phi^2 + \phi^4) dx. \tag{5}$$

Modeling on the nonlinear Schrödinger construction [63,64], we choose the amplitude and width of the oscillon as two collective variables:

$$\phi = A \operatorname{sech}\left(\frac{x}{b}\right). \tag{6}$$

The amplitude $A(t)$ is expected to oscillate between positive and negative values while the width ("breadth") $b(t)$ should remain positive at all times. Substituting the ansatz (6) in (5) gives the Lagrangian of a system with two degrees of freedom:

$$L = \dot{A}^2 b + \left(\frac{1}{3} + \frac{\pi^2}{36}\right) \frac{\dot{b}^2 A^2}{b} + \dot{A}\,\dot{b}\,A - \frac{A^2}{3b} + b\left(\frac{2}{3}A^4 - 4A^2\right). \tag{7}$$

In (7), the overdot stands for the derivative with respect to t. The equations of motion are

$$\ddot{A} + 4A - \left(\frac{1}{3} + \frac{\pi^2}{36}\right) \frac{\dot{b}^2}{b^2} A = \left(2\sigma + \frac{4}{3}\right) A^3 - \left(2\sigma + \frac{1}{3}\right) \frac{A}{b^2} \tag{8a}$$

and

$$\ddot{b} + 2\frac{\dot{A}}{A}\dot{b} = 4\sigma\left(\frac{1}{b^2} - A^2\right) b, \tag{8b}$$

where we have introduced a shorthand notation for a numerical factor

$$\sigma = \frac{1}{1 + \pi^2/3}.$$

B. Asymptotic solution

The system (8) has a family of periodic solutions. For reasons that will become clear in what follows, these solutions are difficult to obtain by means of numerical simulations of Eqs. (8). However, the family can be constructed as a multiscale perturbation expansion—in the limit of small A and large b.

To this end, we let

$$A = \epsilon A_1 + \epsilon^3 A_3 + \cdots, \qquad b = \frac{1}{\epsilon} + \epsilon b_1 + \cdots, \quad (9)$$

where $A_1, A_3, \ldots$ and $b_1, b_3, \ldots$ are functions of a sequence of temporal variables $\mathcal{T}_0, \mathcal{T}_2, \ldots$, with $\mathcal{T}_{2n} = \epsilon^{2n} t$ and $\epsilon \to 0$. Writing $d/dt = \partial/\partial\mathcal{T}_0 + \epsilon^2 \partial\mathcal{T}_2 + \cdots$ and substituting the expansions (9) in (8a), we set coefficients of like powers of ϵ to zero.

The order ϵ^1 gives a linear equation

$$\frac{\partial^2 A_1}{\partial \mathcal{T}_0{}^2} + 4A_1 = 0.$$

Without loss of generality we can take a solution in the form

$$A_1 = \psi e^{2i\mathcal{T}_0} + \text{c.c.} = 2|\psi| \cos 2(\mathcal{T}_0 - \theta), \quad (10)$$

where $\psi = \psi(\mathcal{T}_2, \ldots) = |\psi| e^{-2i\theta}$ is a complex-valued function of "slow" variables. The next order, ϵ^3, gives

$$\frac{\partial^2 A_3}{\partial \mathcal{T}_0{}^2} + 4A_3 = -2\frac{\partial^2 A_1}{\partial \mathcal{T}_0 \partial \mathcal{T}_2} - \left(2\sigma + \frac{1}{3}\right) A_1 + \left(2\sigma + \frac{4}{3}\right) A_1^3. \quad (11)$$

Substituting for A_1 from (10) and imposing the nonsecularity condition

$$4i\frac{\partial \psi}{\partial \mathcal{T}_2} + \left(2\sigma + \frac{1}{3}\right)\psi - (6\sigma + 4)\psi|\psi|^2 = 0, \quad (12)$$

we determine a solution of (11):

$$A_3 = -\frac{1}{8}\left(\sigma + \frac{2}{3}\right)|\psi|^3 \cos 6(\mathcal{T}_0 - \theta). \quad (13)$$

Turning to Eq. (8b), the leading order in its expansion is

$$\frac{\partial^2 b_1}{\partial \mathcal{T}_0{}^2} + \frac{2}{A_1}\frac{\partial A_1}{\partial \mathcal{T}_0}\frac{\partial b_1}{\partial \mathcal{T}_0} = \sigma(1 - A_1^2). \quad (14)$$

The general solution of this linear equation is given by

$$b_1 = \frac{\sigma}{4}(1 - 3|\psi|^2)\tau \tan 2\tau + \frac{\sigma}{16}|\psi|^2 \cos 4\tau + \frac{C_1}{2}\tan 2\tau, \quad (15)$$

where $\tau = \mathcal{T}_0 - \theta$ and C_1 is an arbitrary constant in front of a homogeneous solution. [The second homogeneous solution was absorbed in the term $1/\epsilon$ in the expansion (9).] Letting $C_1 = 0$ and imposing the constraint

$$1 - 3|\psi|^2 = 0 \quad (16)$$

selects a regular solution:

$$b_1 = \frac{\sigma}{48}\cos 4\tau. \quad (17)$$

Finally, the phase of the complex variable ψ is determined by Eq. (12). Substituting $|\psi|$ from (16) we obtain

$$\theta = \frac{1}{8}\mathcal{T}_2.$$

Thus, the asymptotic solution of Eqs. (8) has the form

$$A = \frac{2}{\sqrt{3}}\epsilon \cos \omega t - \frac{3\sigma + 2}{72\sqrt{3}}\epsilon^3 \cos 3\omega t + O(\epsilon^5), \quad (18a)$$

$$b = \frac{1}{\epsilon} + \frac{\sigma}{48}\epsilon \cos 2\omega t + O(\epsilon^3), \quad (18b)$$

where $\epsilon \to 0$ and

$$\omega = 2 - \epsilon^2/4 + O(\epsilon^4).$$

This solution describes a closed orbit in the phase space of the system (8). See Fig. 1.

C. Singular dynamics

It is not difficult to realize that the asymptotic solution (18) is unstable. Indeed, the bounded solution (17) of Eq. (14) is selected by the initial condition $\partial b_1/\partial\mathcal{T}_0 = 0$ at $\mathcal{T}_0 = \theta$. If we, instead, let $\partial b_1/\partial\mathcal{T}_0 = \delta$ with a small δ, the $\tan 2\tau$ component will be turned on in the expression (15) and b_1 will blow up at $\mathcal{T}_0 = \theta + \pi/4$. Figure 1 illustrates the evolution of a small perturbation of the periodic orbit.

The numerical analysis of the system (8) indicates that periodic solutions with $A(t)$ oscillating about zero are unstable for any value of the oscillation amplitude—and not only in the small-A asymptotic regime. The instability originates from the topology of the four-dimensional phase space of the system that features a singularity at $A = 0$.

Indeed, had the system not had a singularity and had the periodic orbit been stable, a small perturbation about it would have been oscillating, quasiperiodically, between positive and negative A. The corresponding trajectory would be winding on a torus in the four-dimensional phase space, with the points where the trajectory passes through $A = 0$ filling a finite interval on the $\dot{b}$ axis. In the presence of the singularity, however, such a torus cannot form because any trajectory crossing through $A = 0$ at time t_* has to satisfy $\dot{b} = 0$ at the same time.

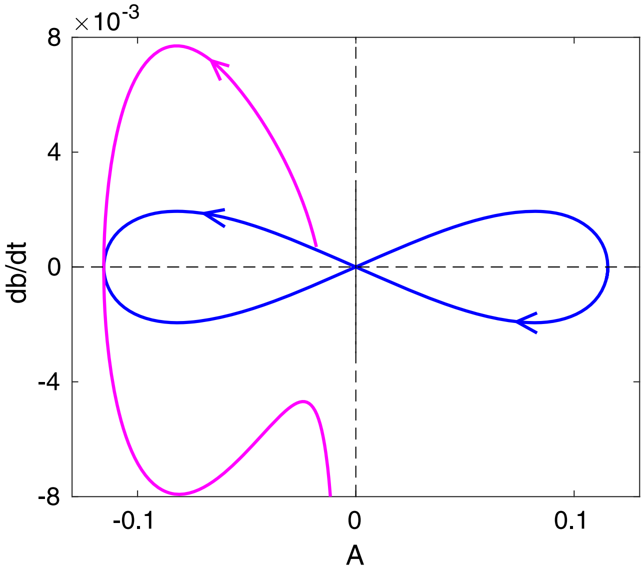

FIG. 1. Trajectories of the four-dimensional system (8) projected on the $(A, \dot{b})$ plane. The ∞-shaped curve describes the periodic solution (18) with $\epsilon = 0.1$. The magenta curve depicts a solution evolving from the initial conditions taken slightly off the periodic trajectory. The initial values $A(0)$, $b(0)$, and $\dot{A}(0)$ for this perturbation are given by the first two terms in Eqs. (18a) and (18b), with $\epsilon = 0.1$ and $t = t_0 = 0.55\pi/\omega$. The initial condition for $\dot{b}$ is $\dot{b}(0) = -\frac{\sigma}{24}\epsilon\omega \sin(2\omega t_0) + 10^{-4}$, with the same ϵ, ω and t_0.

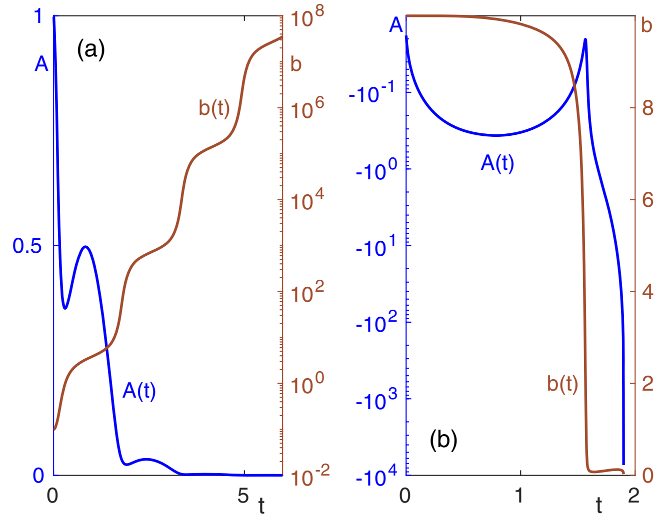

FIG. 2. Two types of unstable evolution in equations (8). (a) $A(t)$ approaches zero while $b(t)$ grows exponentially. (b) $A(t)$ grows to infinity (negative infinity in this simulation) while $b(t)$ shrinks to zero.

Trajectories that do not pass through the plane $A = \dot{b} = 0$ follow one of two scenarios. In the "spreading" scenario, the width $b(t)$ escapes to infinity [Fig. 2(a)]. The corresponding $A(t)$ approaches zero but remains on one side of it at all times. In the alternative scenario, the amplitude $A(t)$ blows up while the width shrinks to zero [Fig. 2(b)].

Because of the singularity of solutions emerging from generic initial conditions, the system (8) is not amenable to the numerical analysis beyond a few oscillation cycles. What is even more important, the all-ω universal instability of periodic solutions of this four-dimensional system does not match up with the behavior of the oscillon solutions of the full partial differential equation (3). Simulations of Eq. (3) demonstrate that, contrary to the predictions of the two-mode approximation, the nearly periodic oscillons with frequencies in the range $\sqrt{2} \lesssim \omega < 2$ are stable. The amplitude and frequency of such oscillons do change due to the third-harmonic radiation; however, these changes are slow and may only be noticeable over long temporal intervals. [See Fig. 3(a).]

We note that an ill-posed system similar to (8) was encountered in the variational studies of the sine-Gordon breathers [67].

The spurious instability of periodic trajectories of the system (8) disqualifies the two-variable ansatz (6) and prompts one to look for suitable alternatives.

III. MULTISCALE VARIATIONAL METHOD

A. Amplitude, width, and phase correction

To rectify the flaws of the "naive" variational algorithm, we consider ϕ to be a function of two time variables, $\mathcal{T}_0 = t$ and $\mathcal{T}_1 = \epsilon t$. The rate of change is assumed to be $O(1)$ on either scale: $\partial\phi/\partial\mathcal{T}_0, \partial\phi/\partial\mathcal{T}_1 \sim 1$. We require ϕ to be periodic in $\mathcal{T}_0$, with a period of T:

$$\phi(\mathcal{T}_0 + T; \mathcal{T}_1) = \phi(\mathcal{T}_0; \mathcal{T}_1).$$

As $\epsilon \to 0$, the variables $\mathcal{T}_0$ and $\mathcal{T}_1$ become independent and the Lagrangian (5) transforms to

$$L = \int \left[\left(\frac{\partial\phi}{\partial\mathcal{T}_0} + \epsilon \frac{\partial\phi}{\partial\mathcal{T}_1} \right)^2 - \phi_x^2 - 4\phi^2 + \phi^4 \right] dx. \tag{19}$$

The action $\int L dt$ is replaced with

$$S = \int_0^T d\mathcal{T}_0 \int d\mathcal{T}_1 L\left(\phi, \frac{\partial\phi}{\partial\mathcal{T}_0}, \frac{\partial\phi}{\partial\mathcal{T}_1}\right). \tag{20}$$

We choose the trial function in the form

$$\phi = A\cos(\omega\mathcal{T}_0 + \theta)\,\mathrm{sech}\left(\frac{x}{b}\right), \tag{21}$$

where A, b, and θ are functions of the "slow" time variable $\mathcal{T}_1$ while $\omega = 2\pi/T$. (Note that ϕ does not have to be assumed small.) The interpretation of the width b is the same as in the ansatz (6) while A represents the maximum of the oscillon's amplitude rather than the amplitude itself. Unlike the previous trial function (6), the variable A in (21)

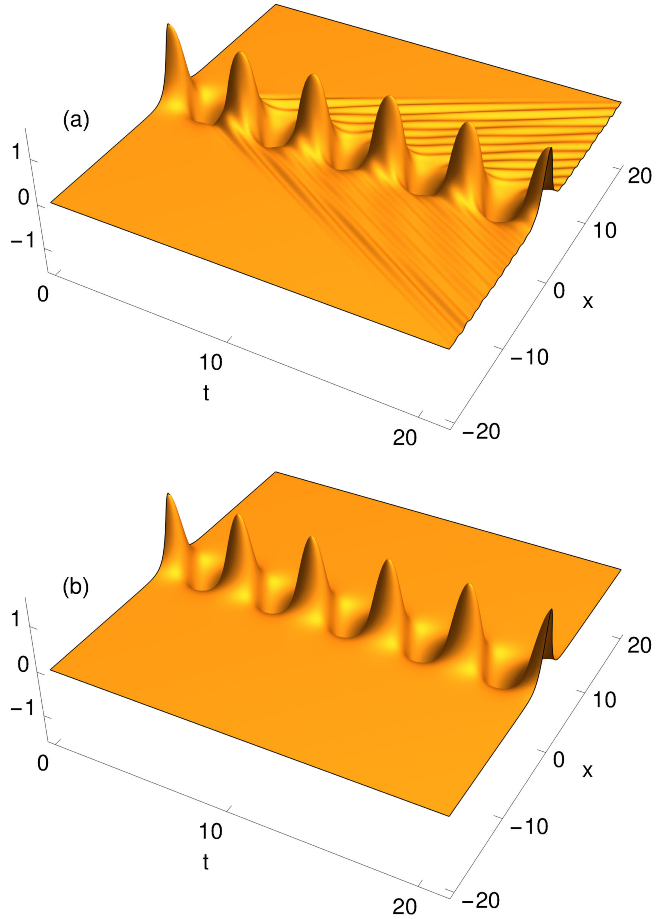

FIG. 3. (a): the Kosevich-Kovalev oscillon with $\omega = 1.06\omega_c$ (where $\omega_c = \sqrt{2}$). The oscillon is stable: despite the energy loss to radiation waves, any changes in its period and amplitude are hardly visible. This figure is obtained by the numerical simulation of Eq. (3). (b): the variational approximation (21) with the matching ω. Here A and b are as in (27) with $\omega = 1.06\omega_c$, and $\theta = 0$. Except for the absence of the radiation waves, the variational pattern is seen to be a good fit for the true oscillon.

is assumed to remain positive at all times. The phase correction θ is a new addition to the set of collective coordinates; its significance will be elucidated later (Sec. IV A). The choice of the spatial part of the ansatz will also be discussed below (Sec. IV B).

Once the explicit dependence on x and $\mathcal{T}_0$ has been integrated away, Eqs. (19) and (20) give an effective action

$$S = T\int d\mathcal{T}_1 \mathcal{L}$$

with

$$\mathcal{L} = (DA)^2 b + \left(\frac{1}{3}+\frac{\pi^2}{36}\right)\frac{(Db)^2A^2}{b} + ADADb + (\omega + D\theta)^2 bA^2 - \frac{A^2}{3b} - 4bA^2 + \frac{1}{2}bA^4 \tag{22}$$

and $D = \epsilon\frac{\partial}{\partial\mathcal{T}_1}$. Two Euler-Lagrange equations are

$$D^2A + 4A - (\omega + D\theta)^2 A - \left(\frac{1}{3}+\frac{\pi^2}{36}\right)\frac{(Db)^2}{b^2}A = \left(1+\frac{3}{2}\sigma\right)A^3 - \left(2\sigma + \frac{1}{3}\right)\frac{A}{b^2} \tag{23}$$

and

$$D[(\omega + D\theta)bA^2] = 0.$$

The last equation can be integrated to give

$$(\omega + D\theta)bA^2 = \ell, \tag{24}$$

where ℓ is a constant of integration. Eliminating the cyclic variable θ between (23) and (24) we arrive at

$$D^2A - \left(\frac{1}{3}+\frac{\pi^2}{36}\right)\frac{(Db)^2}{b^2}A + 4A - \frac{\ell^2}{b^2A^3} = \left(1+\frac{3}{2}\sigma\right)A^3 - \left(2\sigma + \frac{1}{3}\right)\frac{A}{b^2}. \tag{25a}$$

The third Euler-Lagrange equation for the Lagrangian (22) does not involve θ:

$$D^2b + 2\frac{DA}{A}Db = 4\sigma\left(\frac{1}{b^2} - \frac{3}{4}A^2\right)b. \tag{25b}$$

Equations (25) constitute a four-dimensional conservative system with a single control parameter ℓ^2.

B. Slow dynamics and stationary points

The oscillon corresponds to a fixed-point solution of the system (25). There are two coexisting fixed points for each ℓ^2 in the interval $(0, \frac{64}{9})$. We denote their components by (A_+, b_+) and (A_-, b_-), respectively. Here

$$A_\pm^2 = \frac{8}{3} \pm \sqrt{\frac{64}{9} - \ell^2}, \qquad b_\pm^2 = \frac{4}{3}\frac{1}{A_\pm^2}. \tag{26}$$

Turning to the stability of these, we note that all derivatives in Eqs. (25) carry a small factor ϵ. Accordingly, most of the time-dependent solutions of that system evolve on a short scale $\mathcal{T}_1 \sim \epsilon$. This is inconsistent with our original assumption that $\partial\phi/\partial\mathcal{T}_1 = O(1)$. There is, however, a particular ℓ-regime where solutions change slowly and the system (25) is consistent. Specifically, slowly evolving nonstationary solutions can be explicitly constructed in the vicinity of the value $\ell_c^2 = \frac{64}{9}$; see Appendix. This value proves to be a saddle-center bifurcation point separating a branch of stable equilibria, namely (A_-, b_-), from an unstable branch, (A_+, b_+).

Since the asymptotic construction presented in the Appendix is limited to the neighborhood of the bifurcation value ℓ_c, we do not have access to the oscillon perturbations outside that parameter region. Nevertheless, it is not difficult to realize that the two fixed points maintain their stability properties over their entire domain of existence, $0 \le \ell^2 < \ell_c^2$. Indeed, the stability may only change as ℓ passes through the value ℓ_0 given by a root of $\det M = 0$, where M is the linearization matrix. [The evolution is slow and the system (25) is consistent in the vicinity of that point.] There happens to be only one such root and it is given exactly by ℓ_c; see Appendix.

To compare the variational results to conclusions of the direct numerical simulations of Eq. (3), we return to the oscillon ansatz (21). Switching from the parametrization by ℓ to the frequency parameter ω, two branches of fixed points (26) can be characterized in a uniform way:

$$A = \frac{2}{\sqrt{3}}\sqrt{4-\omega^2}, \qquad b = \frac{1}{\sqrt{4-\omega^2}}. \tag{27}$$

[The relations (27) result by letting $\ell = \omega b A^2$ in (26).] The frequencies $\omega_c \le \omega < 2$ correspond to stable oscillons and those in the interval $0 \le \omega < \omega_c$ to unstable ones. Here

$$\omega_c = \sqrt{2}. \tag{28}$$

The third collective coordinate in (21)—the phase correction θ—can be assigned an arbitrary constant value.

Note that the expressions (27) agree with the asymptotic result (4) in the $A, b^{-1} \to 0$ limit.

C. Numerical verification

We simulated the partial differential equation (3) using a pseudospectral numerical scheme with 2^{13} Fourier modes. The scheme imposes periodic boundary conditions $\phi(L) = \phi(-L)$ and $\phi_x(L) = \phi_x(-L)$, where the interval should be chosen long enough to prevent any radiation reentry. (Our L was pegged to the estimated width of the oscillon, varying between $L = 20$ and $L = 100$.)

Using the initial data in the form

$$\phi(x,0) = A_0 \operatorname{sech}\left(\frac{x}{b_0}\right), \qquad \phi_t(x,0) = 0$$

with $b_0 = (2/\sqrt{3})A_0^{-1}$ and varied A_0, we were able to create stable oscillons with frequencies ranging from $\omega = 1.03\omega_c$ to $\omega = 2$. (Here $\omega = 2\pi/T$, where T is the observed period of the localized periodic solution.) This "experimental" stability domain is in good agreement with the variational result $\omega_c \le \omega < 2$.

The 3% discrepancy between two lower threshold values can be attributed to the emission of radiation and the oscillon's core deformation due to the third harmonic excitation. [The presence of the third harmonic in the oscillon's core is manifest already in the asymptotic solution (4).] The radiation intensifies and deformation becomes more significant as the oscillon's amplitude grows [Fig. 3(a)]; yet the variational approximation disregards both effects [see Fig. 3(b)].

Once the evolution has settled to an oscillon with a period T, we would measure its amplitude

$$A = \max_T |\phi(x,t)|_{x=0} \tag{29}$$

and evaluate its width which we define by

$$b = \frac{1}{2A^2} \max_T \int_{-L}^{L} \phi^2(x,t)dx. \tag{30}$$

In (29) and (30), the maximum is evaluated over the time interval $t_0 \le t < t_0 + T$, where t_0 was typically chosen as the position of the third peak of $\phi(0,t)$.

Figure 4 compares the amplitude and width of the numerically generated oscillon with their variational approximations (27). The difference between the numerical and variational results grows as ω approaches $1.03\omega_c$—yet the relative error in the amplitude remains below 8% and the error in the width does not exceed 12.5%.

IV. TWO REMARKS ON THE METHOD

A. Modulation, instability, and significance of θ

The inclusion of the cyclic coordinate $\theta(T_1)$ is crucial for our variational approach. To show that, we compare the

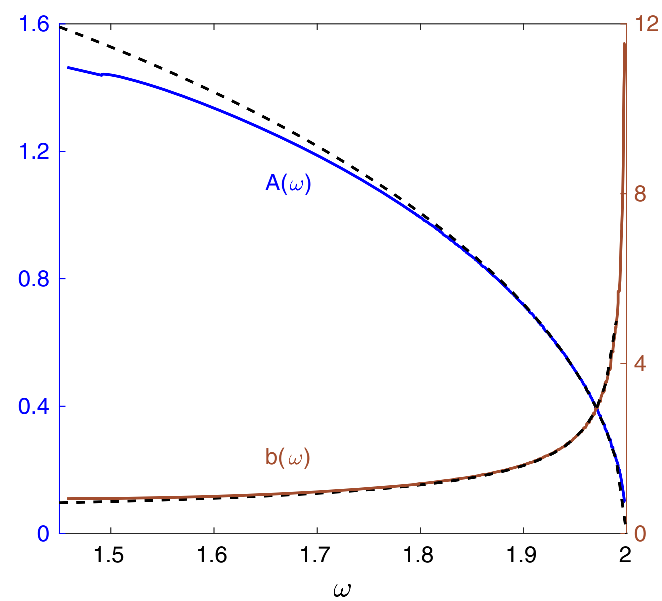

FIG. 4. The amplitude and width of the oscillon as functions of its frequency. The solid curves depict results of the numerical simulations of the partial differential equation (3). The blue curve traces the amplitude-frequency and the brown one gives the width-frequency dependence. The nearby dashed lines describe the corresponding variational approximations (27).

system (25) incorporating, implicitly, 3 degrees of freedom with its 2-degree (A and b) counterpart.

Linearizing Eqs. (25) about the fixed point (27) and considering small perturbations with the time dependence $e^{(\lambda/\epsilon)T_1}$, we obtain a characteristic equation

$$\lambda^4 + (16 - 5A^2 + 3\sigma A^2)\lambda^2 - 18\sigma A^2\left(A^2 - \frac{8}{3}\right) = 0. \quad (31)$$

When A^2 is away from 0 or 8/3, all eigenvalues λ are of order 1. This means that contrary to the assumption under which the system (25) was derived, small perturbations evolve on a short scale $T_1 \sim \epsilon$ rather than $T_1 \sim 1$. The variational method cannot provide trustworthy information on the stability or modulation frequency of the oscillons with those A.

There are two regions where a pair of $O(\epsilon)$ eigenvalues occurs and, consequently, our approach is consistent. One region consists of small $A \sim \epsilon$; this range accounts for the asymptotic regime (4). The second region is defined by $|A^2 - 8/3| = O(\epsilon^2)$ or, equivalently, by $|\omega - \omega_c| \sim \epsilon^2$. As ω is reduced through ω_c, a pair of opposite imaginary eigenvalues converges at the origin and moves onto the positive and negative real axis:

$$\lambda^2 = -\frac{16\sqrt{2}\sigma}{\sigma + 1/3}(\omega - \omega_c) + O((\omega - \omega_c)^2).$$

At this point, a slow modulation of the principal harmonic $\cos(\omega_c t)$ with the modulation frequency $\sim(\omega - \omega_c)^{1/2}$ gives way to an exponential growth of the perturbation. [For an explicit construction of the time-dependent solutions of the system (25), see Appendix.]

Had we not included $\theta(T_1)$ in our trial function—that is, had we set $\theta = 0$ in Eq. (21)—we would have ended up with the same fixed point (27) but a different characteristic equation:

$$\lambda^4 + (3\sigma - 2)A^2\lambda^2 - 9\sigma A^4 = 0. \quad (32)$$

Equation (32) does not have roots of order ϵ outside the asymptotic domain $A \sim \epsilon$. Therefore, the multiscale variational ansatz excluding the cyclic variable $\theta(T_1)$ is inconsistent with the slow evolution of the collective coordinates $A(T_1)$ and $b(T_1)$.

B. Insensitivity to spatial shape variations

The x part of the trial function (21) was chosen so as to reproduce the asymptotic representation (4) and match the amplitude-frequency relationship as $\omega \to 2$. As for the global behavior of the $A(\omega)$ curve, the variation of the spatial profile of the trial function has little effect on it—as long as the function remains localized.

To exemplify this insensitivity to the ansatz variations, we replace the exponentially localized trial function (21) with a Gaussian:

$$\phi = A\cos(\omega\mathcal{T}_0 + \theta)e^{-(x/b)^2}. \quad (33)$$

As in (21), the amplitude A, width b, and phase shift θ are assumed to be functions of the slow time variable $\mathcal{T}_1 = \epsilon t$. Substituting in (20) gives an effective action with the Lagrangian

$$\mathcal{L} = (DA)^2 b + \frac{3}{4}\frac{(Db)^2A^2}{b} + ADADb + (\omega + D\theta)^2 bA^2 - \frac{A^2}{b} - 4bA^2 + \frac{3\sqrt{2}}{8}bA^4. \quad (34)$$

(Here, as before, $D = \epsilon\partial/\partial T_1$.) Equation (34) has the same form as (22) with the only difference residing in the value of some of the coefficients.

The Euler-Lagrange equations resulting from (34) have a fixed-point solution

$$A = \frac{2^{7/4}}{3}\sqrt{4 - \omega^2}, \qquad b = \frac{1}{\sqrt{3}}\frac{1}{\sqrt{4 - \omega^2}}. \quad (35)$$

Note that the Gaussian amplitude and width are related to ω by exactly the same laws as the amplitude and width of the secant-shaped approximation [Eqs. (27)]. If A_g stands for the amplitude (35) and A_s for the secant-based result (27), the ratio $A_g(\omega)/A_s(\omega)$ is given by $\sqrt[4]{8/9} \approx 0.971$. Thus the Gaussian-based amplitude-frequency curve reproduces the qualitative behavior of the curve (27), with the Gaussian amplitude being only 3% different from the amplitude of the secant-shaped variational oscillon.

Linearizing the Euler-Lagrange equations about the fixed point (35) we obtain a Gaussian analog of the characteristic equation (31):

$$\lambda^4 + \left(16 - \frac{27\sqrt{2}}{8}A^2\right)\lambda^2 - \frac{27}{8}A^2\left(A^2 - \frac{32}{9\sqrt{2}}\right) = 0. \quad (36)$$

The critical value of A^2 above which a pair of opposite eigenvalues moves onto the real axis is $32/9\sqrt{2}$. Remarkably, the corresponding threshold frequency $\omega_c = \sqrt{2}$ coincides with the value (28) afforded by the secant ansatz.

V. CONCLUSIONS

This study was motivated by the numerous links and similarities between the Klein-Gordon oscillons and solitons of the nonlinear Schrödinger equations. A simple yet powerful approach to the Schrödinger solitons exploits the variation of action. By contrast, the variational analysis of the Klein-Gordon oscillons has not been nearly as successful.

One obstacle to the straightforward ("naive") variational treatment of the oscillon is that its width proves to be unsuitable as a collective coordinate in that approach. The soliton's amplitude and width comprise a standard choice of variables in the Schrödinger domain, but making a similar choice in the Klein-Gordon Lagrangian results in a singular four-dimensional system.

This paper presents a variational method free from singularities. The method aims at determining the oscillon's parameters, domain of existence, and stability-instability transition points. The proposed formulation is based on a fast harmonic ansatz supplemented by the adiabatic evolution of the oscillon's collective coordinates. An essential component of the set of collective coordinates is the "lazy phase": a cyclic variable accounting for nonuniform phase acquisitions.

We employed the Kosevich-Kovalev model as a prototype equation exhibiting oscillon solutions. Our variational method establishes the oscillon's domain of existence ($0 < \omega < 2$) and identifies the frequency ω_c at which the oscillon loses its stability ($\omega_c = \sqrt{2}$). The predicted stability domain is in good agreement with numerical simulations of the partial differential equation (3) which yield stable oscillons with frequencies $1.03\omega_c \leq \omega < 2$. The variational amplitude-frequency and width-frequency curves are consistent with the characteristics of the numerical solutions.

ACKNOWLEDGMENTS

Discussions with Alexander Kovalev are gratefully acknowledged. This study was supported by a collaboration grant from the National Research Foundation of South Africa and Joint Institute for Nuclear Research (NRF Grant No. 120467).

APPENDIX: SLOW EVOLUTION NEAR THE ONSET OF INSTABILITY

The aim of this appendix is to construct a slowly changing solution of the system (25) consistent with the assumption used in the derivation of that system. The construction is carried out in the vicinity of the parameter value signifying the onset of instability of the fixed point.

We let

$$\ell^2 = \ell_0^2 - \epsilon^4, \tag{A1}$$

where ℓ_0 is the parameter value to be determined. The unknowns are expanded as

$$\begin{aligned} A &= A_0 + \epsilon^2 A_1 + \epsilon^4 A_2 + \cdots, \\ b &= b_0 + \epsilon^2 b_1 + \epsilon^4 b_2 + \cdots. \end{aligned} \tag{A2}$$

Here (A_0, b_0) is either of the two fixed points (26) corresponding to $\ell = \ell_0$. Substituting (A1) and (A2) in (25) we equate coefficients of like powers of ϵ.

The order ϵ^2 gives

$$M\vec{Y}_1 = 0,$$

where the matrix M has the form

$$\begin{pmatrix} 4 + \frac{9\ell_0^2}{4A_0^2} - \frac{11+12\sigma}{4} A_0^2 & \left[\frac{3}{2}\frac{\ell_0^2}{A_0^2} - \frac{1+6\sigma}{2} A_0^2\right]\frac{A_0}{b_0} \\ 6\sigma A_0 b_0 & 6\sigma A_0^2 \end{pmatrix} \tag{A3}$$

and the vector $\vec{Y}_1$ consists of the linearized perturbations of the fixed point:

$$\vec{Y}_1 = \begin{pmatrix} A_1 \\ b_1 \end{pmatrix}.$$

Setting $\det M = 0$ determines the value of ℓ_0^2. This value turns out to coincide with ℓ_c^2, the end point of the interval of existence of the fixed points:

$$\ell_0^2 = \ell_c^2 = \frac{64}{9}. \tag{A4}$$

As ℓ approaches ℓ_c, the fixed points (A_+, b_+) and (A_-, b_-) join to become (A_c, B_c). Here

$$A_c = \sqrt{\frac{8}{3}}, \qquad b_c = \frac{1}{\sqrt{2}}. \tag{A5}$$

The components of the null eigenvector $\vec{Y}_1$ are readily identified:

$$A_1 = A_c y, \qquad b_1 = -b_c y.$$

Here $y = y(\mathcal{T}_1)$ is an arbitrary scalar function that will be determined at the next order of the expansion.

At the order ϵ^4 we obtain

$$M\vec{Y}_2 = \vec{F}_2, \tag{A6}$$

where

$$\vec{F}_2 = \begin{pmatrix} f_2 \\ g_2 \end{pmatrix}$$

with

$$\begin{aligned} f_2 &= -A_c \partial_1^2 y + 8A_c\left(\frac{4}{3} - \sigma\right)y^2 - \frac{1}{A_c^3 b_c^2}, \\ g_2 &= b_c \partial_1^2 y + 16\sigma b_c y^2. \end{aligned}$$

The solvability condition for Eq. (A6) is

$$\vec{Z} \cdot \vec{F}_2 = 0, \tag{A7}$$

where

$$\vec{Z} = \begin{pmatrix} A_c b_c \\ \frac{4}{3}\left(1 - \frac{1}{3\sigma}\right) \end{pmatrix}$$

is the adjoint null eigenvector of the matrix M. Substituting for A_c and b_c from (A5), Eq. (A7) yields

$$\left(1 + \frac{1}{3\sigma}\right)\partial_1^2 y = 16y^2 - \frac{9}{16}. \tag{A8}$$

The amplitude equation (A8) has the form of the second Newton's law for a classical particle moving in the potential

$$U(y) = \frac{9}{16}y - \frac{16}{3}y^3.$$

The potential has two equilibria: a minimum at $y_- = -\frac{3}{16}$ and a maximum at $y_+ = \frac{3}{16}$. These correspond to the two fixed points of the system (25): the minimum pertains to (A_-, b_-) and the maximum to (A_+, b_+). Accordingly, the point (A_-, b_-) is stable and (A_+, b_+) unstable.

The stable fixed point is surrounded by a family of closed orbits. The corresponding periodic solutions of Eq. (A8) are expressible in Jacobi functions:

$$y(\mathcal{T}_1) = -\frac{k^2+1}{3}\mu + k^2\mu \,\mathrm{sn}^2\left(\sqrt{\frac{8\sigma\mu}{1+3\sigma}}\mathcal{T}_1, k\right),$$

where

$$\mu = \frac{9}{16}\sqrt{\frac{k^2+1}{k^6+1}}.$$

The elliptic modulus k, $0 \le k \le 1$, serves as the parameter of the family.

[1] E. J. Copeland, M. Gleiser, and H.-R. Müller, Oscillons: Resonant configurations during bubble collapse, Phys. Rev. D **52**, 1920 (1995).

[2] A. Riotto, Oscillons are not present during a first order electroweak phase transition, Phys. Lett. B **365**, 64 (1996).

[3] I. Dymnikova, L. Koziel, M. Khlopov, and S. Rubin, Quasilumps from first order phase transitions, Gravitation Cosmol. **6**, 311 (2000).

[4] M. Broadhead and J. McDonald, Simulations of the end of supersymmetric hybrid inflation and nontopological soliton formation, Phys. Rev. D **72**, 043519 (2005).

[5] M. Gleiser, Oscillons in scalar field theories: Applications in higher dimensions and inflation, Int. J. Mod. Phys. D **16**, 219 (2007).

[6] E. Farhi, N. Graham, A. H. Guth, N. Iqbal, R. R. Rosales, and N. Stamatopoulos, Emergence of oscillons in an expanding background, Phys. Rev. D **77**, 085019 (2008).

[7] M. Gleiser, B. Rogers, and J. Thorarinson, Bubbling the false vacuum away, Phys. Rev. D **77**, 023513 (2008).

[8] M. A. Amin, Inflaton fragmentation: Emergence of pseudo-stable inflaton lumps (oscillons) after inflation, arXiv:1006.3075.

[9] M. Gleiser, N. Graham, and N. Stamatopoulos, Generation of coherent structures after cosmic inflation, Phys. Rev. D **83**, 096010 (2011).

[10] M. A. Amin, R. Easther, H. Finkel, R. Flauger, and M. P. Hertzberg, Oscillons after inflation, Phys. Rev. Lett. **108**, 241302 (2012).

[11] S.-Y. Zhou, E. J. Copeland, R. Easther, H. Finkel, Z.-G. Moua, and P. M. Saffin, Gravitational waves from oscillon preheating, J. High Energy Phys. 10 (2013) 026.

[12] M. Gleiser and N. Graham, Transition to order after hilltop inflation, Phys. Rev. D **89**, 083502 (2014).

[13] P. Adshead, J. T. Giblin Jr., T. R. Scully, and E. I. Sfakianakis, Gauge-preheating and the end of axion inflation, J. Cosmol. Astropart. Phys. 12 (2015) 034.

[14] J. R. Bond, J. Braden, and L. Mersini-Houghton, Cosmic bubble and domain wall instabilities III: The role of oscillons in three-dimensional bubble collisions, J. Cosmol. Astropart. Phys. 09 (2015) 004.

[15] S. Antusch, F. Cefalà, and S. Orani, Gravitational waves from oscillons after inflation, Phys. Rev. Lett. **118**, 011303 (2017).

[16] J.-P. Hong, M. Kawasaki, and M. Yamazaki, Oscillons from pure natural inflation, Phys. Rev. D **98**, 043531 (2018).

[17] K. D. Lozanov and M. A. Amin, Gravitational perturbations from oscillons and transients after inflation, Phys. Rev. D **99**, 123504 (2019).

[18] D. Cyncynates and T. Giurgica-Tiron, Structure of the oscillon: The dynamics of attractive self-interaction, Phys. Rev. D **103**, 116011 (2021).

[19] V. A. Koutvitsky and E. M. Maslov, Gravipulsons, Phys. Rev. D **83**, 124028 (2011); Passage of test particles through oscillating spherically symmetric dark matter configurations, Phys. Rev. D **104**, 124046 (2021).

[20] H.-Y. Zhang, Gravitational effects on oscillon lifetimes, J. Cosmol. Astropart. Phys. 03 (2021) 102.

[21] Z. Nazari, M. Cicoli, K. Clough, and F. Muia, Oscillon collapse to black holes, J. Cosmol. Astropart. Phys. 05 (2021) 027.

[22] X.-X. Kou, C. Tian, and S.-Y. Zhou, Oscillon preheating in full general relativity, Classical Quantum Gravity **38**, 045005 (2021).

[23] T. Hiramatsu, E. I. Sfakianakis, and M. Yamaguchi, Gravitational wave spectra from oscillon formation after inflation, J. High Energy Phys. 03 (2021) 021.

[24] X.-X. Kou, J. B. Mertens, C. Tian, and S.-Y. Zhou, Gravitational waves from fully general relativistic oscillon preheating, Phys. Rev. D **105**, 123505 (2022).

[25] E. W. Kolb and I. I. Tkachev, Nonlinear axion dynamics and the formation of cosmological pseudosolitons, Phys. Rev. D **49**, 5040 (1994).

[26] A. Vaquero, J. Redondo, and J. Stadler, Early seeds of axion miniclusters, J. Cosmol. Astropart. Phys. 04 (2019) 012.

[27] M. Kawasaki, W. Nakanoa, and E. Sonomoto, Oscillon of ultra-light axion-like particle, J. Cosmol. Astropart. Phys. 01 (2020) 047.

[28] J. Olle, O. Pujolas, and F. Rompineve, Oscillons and dark matter, J. Cosmol. Astropart. Phys. 02 (2020) 006.

[29] A. Arvanitaki, S. Dimopoulos, M. Galanis, L. Lehner, J. O. Thompson, and K. Van Tilburg, Large-misalignment mechanism for the formation of compact axion structures: Signatures from the QCD axion to fuzzy dark matter, Phys. Rev. D **101**, 083014 (2020).

[30] M. Kawasaki, K. Miyazaki, K. Murai, H. Nakatsuka, and E. Sonomoto, Anisotropies in cosmological 21 cm background by oscillons/ I-balls of ultra-light axion-like particle, J. Cosmol. Astropart. Phys. 08 (2022) 066.

[31] S. Antusch, F. Cefalà, S. Krippendorf, F. Muia, S. Orani, and F. Quevedo, Oscillons from string moduli, J. High Energy Phys. 01 (2018) 083.

[32] Y. Sang and Q.-G. Huang, Stochastic gravitational-wave background from axion-monodromy oscillons in string theory during preheating, Phys. Rev. D **100**, 063516 (2019).

[33] S. Kasuya, M. Kawasaki, F. Otani, and E. Sonomoto, Revisiting oscillon formation in the Kachru-Kallosh-Linde-Trivedi scenario, Phys. Rev. D **102**, 043016 (2020).

[34] E. Farhi, N. Graham, V. Khemani, R. Markov, and R. Rosales, An oscillon in the SU(2) gauged Higgs model, Phys. Rev. D **72**, 101701(R) (2005).

[35] N. Graham, An electroweak oscillon, Phys. Rev. Lett. **98**, 101801 (2007); Numerical simulation of an electroweak oscillon, Phys. Rev. D **76**, 085017 (2007).

[36] M. Gleiser, N. Graham, and N. Stamatopoulos, Long-lived time-dependent remnants during cosmological symmetry breaking: From inflation to the electroweak scale, Phys. Rev. D **82**, 043517 (2010).

[37] E. I. Sfakianakis, Analysis of oscillons in the SU(2) gauged Higgs model, arXiv:1210.7568.

[38] M. Gleiser and J. Thorarinson, Phase transition in U(1) configuration space: Oscillons as remnants of vortex-antivortex annihilation, Phys. Rev. D **76**, 041701(R) (2007).

[39] V. Achilleos, F. K. Diakonos, D. J. Frantzeskakis, G. C. Katsimiga, X. N. Maintas, E. Manousakis, C. E. Tsagkarakis, and A. Tsapalis, Oscillons and oscillating kinks in the Abelian-Higgs model, Phys. Rev. D **88**, 045015 (2013).

[40] N. A. Voronov, I. Y. Kobzarev, and N. B. Konyukhova, Possibility of the existence of X mesons of a new type, JETP Lett. **22**, 290 (1975).

[41] I. L. Bogolyubskii and V. G. Makhankov, On the pulsed soliton lifetime in two classical relativistic theory models, JETP Lett. **24**, 12 (1976).

[42] I. L. Bogolyubskii and V. G. Makhankov, Dynamics of spherically symmetrical pulsons of large amplitude, JETP Lett. **25**, 107 (1977).

[43] M. Gleiser, Pseudostable bubbles, Phys. Rev. D **49**, 2978 (1994).

[44] R. Rajaraman, *Solitons and Instantons* (North-Holland, Amsterdam, 1982).

[45] N. Manton and P. Sutcliffe, *Topological Solitons* (Cambridge University Press, Cambridge, England, 2004).

[46] E. J. Weinberg, *Classical Solutions in Quantum Field Theory* (Cambridge University Press, Cambridge, England, 2012).

[47] S. Rychkov and L. G. Vitale, Hamiltonian truncation study of the ϕ^4 theory in two dimensions. II. The $\mathbb{Z}_2$ -broken phase and the Chang duality, Phys. Rev. D **93**, 065014 (2016).

[48] Z. Bajnok and M. Lajer, Truncated Hilbert space approach to the 2d ϕ^4 theory, J. High Energy Phys. 10 (2016) 050.

[49] M. Serone, G. Spada, and G. Villadoro, $\lambda\phi^4$ theory—Part II. The broken phase beyond NNNN(NNNN)LO, J. High Energy Phys. 05 (2019) 047.

[50] N. Graham and H. Weigel, Quantum corrections to soliton energies, Int. J. Mod. Phys. A **37**, 2241004 (2022).

[51] M. A. A. Martin, R. Schlesier, and J. Zahn, The semiclassical energy density of kinks and solitons, Phys. Rev. D **107**, 065002 (2023).

[52] H. Ito and M. Kitazawa, Gravitational form factors of a kink in $1+1$ dimensional ϕ^4 model, J. High Energy Phys. 08 (2023) 033.

[53] R. Maxton and Y. Meurice, Perturbative boundaries of quantum advantage: Real-time evolution for digitized $\lambda\phi^4$ lattice models, Phys. Rev. D **107**, 074508 (2023).

[54] A. Vilenkin and E. P. S. Shellard, *Cosmic Strings and Other Topological Defects* (Cambridge University Press, Cambridge, England, 1994).

[55] G. Fodor, A review on radiation of oscillons and oscillatons, arXiv:1911.03340.

[56] G. Fodor, P. Forgács, Z. Horváth, and Á. Lukács, Small amplitude quasibreathers and oscillons, Phys. Rev. D **78**, 025003 (2008).

[57] G. Fodor, P. Forgács, Z. Horváth, and M. Mezei, Computation of the radiation amplitude of oscillons, Phys. Rev. D **79**, 065002 (2009).

[58] E. P. Honda and M. W. Choptuik, Fine structure of oscillons in the spherically symmetric φ^4 Klein-Gordon model, Phys. Rev. D **65**, 084037 (2002).

[59] M. Gleiser and M. Krackow, Configurational entropic study of the enhanced longevity in resonant oscillons, Phys. Lett. B **805**, 135450 (2020).

[60] G. Fodor, P. Forgácz, P. Grandclément, and I. Rácz, Oscillons and quasibreathers in the ϕ^4 Klein-Gordon model, Phys. Rev. D **74**, 124003 (2006).

[61] N. V. Alexeeva, I. V. Barashenkov, A. A. Bogolubskaya, and E. V. Zemlyanaya, Understanding oscillons: Standing waves in a ball, Phys. Rev. D **107**, 076023 (2023).

[62] P. G. Kevrekidis, R. Carretero-González, J. Cuevas-Maraver, D. J. Frantzeskakis, J.-G. Caputo, and B. A. Malomed, Breather stripes and radial breathers of the two-dimensional sine-Gordon equation, Commun. Nonlinear Sci. Numer. Simul. **94**, 105596 (2021).

[63] B. A. Malomed, Variational methods in nonlinear fiber optics and related fields, Prog. Opt. **43**, 71 (2002).

[64] I. V. Barashenkov, N. V. Alexeeva, and E. V. Zemlyanaya, Two- and three-dimensional oscillons in nonlinear Faraday resonance, Phys. Rev. Lett. **89**, 104101 (2002).

[65] A. M. Kosevich and A. S. Kovalev, Self-localization of vibrations in a one-dimensional anharmonic chain, Sov. Phys. JETP **40**, 891 (1975).

[66] J. A. D. Wattis, Variational approximations to breather modes in the discrete sine-Gordon equation, Physica (Amsterdam) **82D**, 333 (1995).

[67] J. G. Caputo and N. Flytzanis, Kink-antikink collisions in sine-Gordon and ϕ^4 models: Problems in the variational approach, Phys. Rev. A **44**, 6219 (1991).